Heat Transfer to Non-Newtonian Fluids in Transitional and Turbulent Flow

A. W. PETERSEN and E. B. CHRISTIANSEN

University of Utah, Salt Lake City, Utah

Turbulent and transitional flow heat transfer correlations for non-Newtonian fluids are presented. By means of an extension of the Reichardt-Metzner-Friend correlation to nonisothermal flow, and a new definition of Prandtl number to account for deviations from Newtonian behavior, turbulent flow data are correlated to a standard deviation of 14.8%. By means of a normalizing procedure, data for the complex case of transitional flow heat transfer to non-Newtonian fluids are correlated to a standard deviation of 17.7%. At the transition region boundaries, the correlation is consistent with laminar and turbulent flow correlations. A basic similarity in the Newtonian and non-Newtonian heat transfer mechanisms is suggested.

A theoretical analogy by Reichardt (*44*) for heat transfer in turbulent flow in pipes has been improved by Metzner and W. L. Friend (*17, 18*) and has been extended to non-Newtonian fluids by Metzner and P. S. Friend (*36*). The correlation equation of Metzner and P. S. Friend has the disadvantage of being restricted to nearly isothermal flow heat transfer, since no allowance is made for the effect of temperature profile on physical properties. In addition, it is empirically shown below that predictions of the above correlation equation deviate increasingly from experimental data on pseudoplastic fluids for increasing deviations from Newtonian behavior. In the work below, the correlation of Metzner and Friend is extended to the case of highly nonisothermal flow, and it is shown that a redefinition of the Prandtl number accounts for the effect of increasingly non-Newtonian behavior.

There has been little success in correlating transitional flow heat transfer data for non-Newtonian fluids (*3, 9, 33, 34, 38, 54*). The difficulty has been in accounting for the change of heat transfer mechanism with flow rate, and in defining variables which account for the local variation of viscosity with both flow rate and radial position in the pipe. In the presently reported research, a heat transfer correlation for the transition region is developed by means of a normalizing procedure. A variable, which is a function only of the Reynolds number, is derived to account for the changing heat transfer mechanism in the transition region.

The discussion on non-Newtonian fluids will be limited to the common types: pseudoplastic and Bingham plastic. The shear stress-strain rate relationship for pseudoplastic fluids is assumed to be represented approximately by the equation

$$\tau = K\dot{S}^n \tag{1}$$

and for Bingham plastic fluids, by the equation

$$\tau = \tau_y + \eta\dot{S} \tag{2}$$

The effect of deviations from Equation (1) may be reduced by the evaluation of n and K at the τ_w in the range of the variable to be considered; for example, $(N_{Re})_{wc}$ should be based upon the value of n at τ_{wc}.

A. W. Petersen is with Stauffer Chemical Company, Salt Lake City, Utah.

TURBULENT FLOW CORRELATION

The correlation of Metzner and Friend (*36*) for non-Newtonian fluids may be written as

$$N_{St} = \frac{\left(\frac{f}{2\,\theta_m}\right)}{\frac{1}{\phi_m} + 11.8\sqrt{\frac{f}{2}}\,\frac{[(N_{Pr})_w - 1]}{(N_{Pr})_w^{1/3}}} \tag{3}$$

The form of Equation (3) was obtained by Metzner and Friend from the theoretical work of Reichardt (*44*), who derived a correlation for Newtonian fluids with the use of the analogy between heat and momentum transfer. Reichardt showed that the assumptions for his analogy were valid for $N_{Re}N_{Pr} > 2{,}500$. Metzner and Friend extended the Newtonian fluid correlation to the non-Newtonian fluid case by defining the Prandtl number at the shear stress conditions existing at the pipe wall.

Equation (3) is restricted to a low temperature difference driving force. Metzner and Friend (*35*) suggested the use of the correction of Kreith and Summerfield (*28*), $(\mu_w/\mu_b)^{0.110}$, or the correction of Sieder and Tate (*47*), $(\mu_w/\mu_b)^{0.14}$, to extend the Newtonian analog of Equation (3) to the nonisothermal case. The heat transfer data for water of this work (*40*) and Friend (*16*), plotted in Figure 1, are best correlated when the following quantities

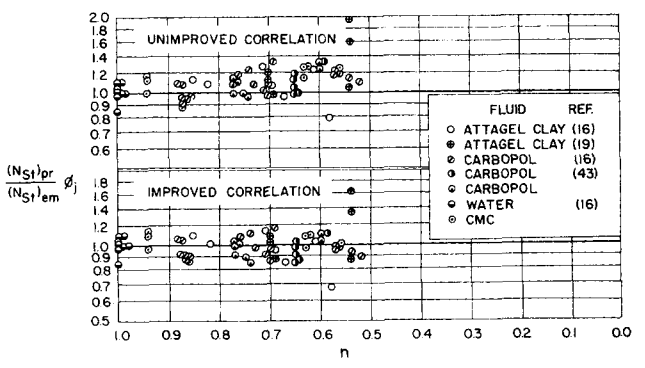

Fig. 1. Ratio of predicted to experimental turbulent flow heat transfer rate with different Prandtl number definitions.

are used in Equation (3): $(\mu_w/\mu_b)^{0.10}$, the Prandtl number $(N_{Pr})_b$ evaluated at the bulk fluid temperature, and the friction factor f_i that would be obtained if flow were isothermal at the bulk fluid temperature. Substitution into Equation (3) of the analogous quantities for non-Newtonian fluids, $(\mu_{ww}/\mu_{wb})^{0.10}$, $(N_{Pr})_{wb}$, and f_i, results in the equation

$$N_{St} = \frac{\left(\frac{f_i}{2\,\theta_m}\right)\left(\frac{\mu_{ww}}{\mu_{wb}}\right)^{-0.10}}{\frac{1}{\phi_m} + 11.8\sqrt{\frac{f_i}{2}}\,\frac{[(N_{Pr})_{wb}-1]}{(N_{Pr})_{wb}^{1/3}}} \qquad (4)$$

which should be the nonisothermal flow extension of Equation (3) for both Newtonian and non-Newtonian flow.

Trend with Non-Newtonian Behavior

Equation (4) was tested with the turbulent and transitional flow heat transfer data of Friend (*16*), Haines (*19*), Raniere (*43*), and this work (*40*) taken with pseudoplastic fluids, as shown in Figure 1 (*top*). Some transitional flow data, distinguished by having a flow rate less than (10,000/2,100) times the critical flow rate, are included in Figure 1, because insufficient fully turbulent flow data are available at low values of n. These were converted to turbulent flow conditions by dividing the N_{St} by an estimated ϕ_j factor. The ϕ_j factor is defined in the Transitional Flow Correlation section. To minimize any uncertainty in this procedure, only transitional flow data with ϕ_j in the range 0.95 to 1.00 (a correction of less than 6% in N_{St}) were used.

The quantity f_i was calculated from the measured f_{ni} by means of the non-Newtonian analog of the Sieder-Tate (*47*) equation with the 1.02 factor omitted

$$f_i = f_{ni}\,(\mu_{ww}/\mu_{wb})^{-0.10} \qquad (5)$$

except in cases (*18*) where f_i was measured in an isothermal flow section in series with the test section.

It may be noted that there is a definite trend of the data with n in Figure 1 (*top*). The arithmetical average deviation of the data from the line $(N_{St})_{pr}\,\phi_j/(N_{St})_{em} = 1$ is + 11.9%, and the standard deviation is 21.7%.

Correction for Trend with Non-Newtonian Behavior

Compensation for the trend of the data with n is made by an increase in the effective Prandtl number in Equation (4). Qualitatively, increasing the Prandtl number is reasonable because the viscosity in the low shear rate central region of the pipe, as n decreases, becomes increasingly larger than the wall viscosity in the $(N_{Pr})_{wb}$ used in Equation (4). Even though most of the heat transfer resistance is near the wall, the use of $(N_{Pr})_{wb}$ in Equation (4) is not strictly correct and a slightly larger value for the effective Prandtl number should be used for $n < 1$.

A similar effect of higher viscosity in the central part of the pipe is observed in the retardation of the onset of turbulence in comparison with a Newtonian fluid. As shown in Figure 6, the critical Reynolds number based upon μ_{wb}, $(N_{Re})_{wc}$, is greater than the 2,100 for Newtonian fluids.

An effective viscosity μ_e, larger than μ_{wb}, may be defined such that the critical Reynolds number is equal to 2,100 for non-Newtonian flow also.

$$(DU\rho/\mu_e)_c = 2{,}100 \qquad (6)$$

Multiplication of the left side of Equation (6) by μ_{wb}/μ_{wb} and substitution for the definition of $(N_{Re})_{wc}$ yield

$$\mu_e = \mu_{wb}[(N_{Re})_{wc}/2{,}100] \qquad (7)$$

It is proposed that the same μ_e that normalizes the critical Reynolds number to 2,100 be used in the Prandtl number definition to yield a Prandtl number more characteristic of a non-Newtonian fluid. The resulting effective N_{Pr} is

$$N_{Pr} = (N_{Pr})_{wb}\,[(N_{Re})_{wc}/2{,}100] \qquad (8)$$

With the definition of N_{Pr} given by Equation (8), the final correlation for heat transfer to pseudoplastic fluids in turbulent flow becomes

$$N_{St} = \frac{\left(\frac{f_i}{2\,\theta_m}\right)\left(\frac{\mu_{ww}}{\mu_{wb}}\right)^{-0.10}}{\frac{1}{\phi_m} + 11.8\sqrt{\frac{f_i}{2}}\,\frac{[N_{Pr}-1]}{(N_{Pr})^{1/3}}} \quad \text{(pseudoplastic)} \qquad (9)$$

A plot of f_i is given in Figure 8. The variables N_{Re}, N_{Pr}, θ_m, ϕ_m, and $(\mu_{ww}/\mu_{wb})^{-0.10}$ are evaluated by methods developed in the section on Calculation of Variables.

The analogous equation for Bingham plastic fluids is

$$N_{St} = \frac{\left(\frac{f_i}{2\,\theta_m}\right)\left(\frac{\eta_w}{\eta_b}\right)^{-0.10}}{\frac{1}{\phi_m} + 11.8\sqrt{\frac{f_i}{2}}\,\frac{[N_{Pr}-1]}{(N_{Pr})^{1/3}}} \quad \text{(Bingham plastic)} \qquad (10)$$

The $(N_{Re})_{wc}/2{,}100$ factor is difficult to apply to the definition of N_{Pr} for a Bingham plastic fluid where n is not constant. The n near the wall is close to 1.0 for turbulent flow of Bingham plastics, even for fluids with a large N_{He}. Since the equivalent of $(N_{Re})_{wc}/2{,}100$ would also be approximately 1.0, the Prandtl number in the turbulent region is taken as approximately

$$N_{Pr} = (N_{Pr})_{\eta b} \quad \text{(Bingham plastic)} \qquad (11)$$

Equations (9) and (10) apply only for $N_{Re} > 10{,}000$. For $N_{Re} = 2{,}100$ to 10,000, Equation (24) for transitional flow must be used.

Results and Discussion

The arithmetical average deviation of the data from the predictions using the effective N_{Pr} in place of $(N_{Pr})_{wb}$ is + 1.2% for the data plotted in Figure 1 (*bottom*), and the standard deviation is 14.8%. The small average deviation of the experimental data from the prediction of Equation (9) and the reasonable standard deviation justify the modified definition of N_{Pr} given in Equation (8).

A test of the Bingham plastic equation is not shown, but it may be seen in Figure 5 that transitional flow data near the turbulent region are adequately correlated by means of Equation (10), which is represented by the solid curve at $N_{Re} = 10{,}000$.

The treatment of the Friend–Haines–Raniere data used in this work differed from that by Metzner and Friend (*36*). In an effort to reduce the standard deviation of these data, the following procedures were employed:

1. Transitional flow data points with large deviations from turbulent flow conditions ($\phi_j < 0.95$) were not used.
2. All other transitional flow data points were corrected to equivalent turbulent flow conditions with the ϕ_j factor.
3. A few sets of data with obvious inconsistencies were not used.
4. A few minor corrections, such as for temperature effects, were made.

The data of Farmer (*15*) were not used because of the unavailability of a thesis. The data originally used by Metzner and Friend were correlated by Equation (3)

with a standard deviation of 23.5% (36). With all of the differences in treatment listed above, the standard deviation was reduced only to 22.6%. But the redefinition of N_{Pr} resulted in the significant lowering of the standard deviation to 16.2%.

EQUIPMENT AND CALIBRATIONS

The rheological data were measured by a 1/16-in. diameter capillary tube viscometer with an L/D of 290 or by a rotary viscometer with a 3-in. diameter cup and a 1/16-in. clearance. Both instruments were calibrated with a 60% sucrose solution and a Bureau of Standards oil. Shear stress–shear rate data, given completely in reference *40*, were taken at two temperatures to find $\Delta H^{\neq}/R$ and at twice daily to allow linear interpolation of the rheogram to account for an irreversible decrease in viscosity due to heating and shearing.

The heat transfer data were taken in 1-, 1½-, and 2-in. standard copper pipe with 15-ft. calming sections followed by successive 10-, 4¾-, 2¼-, and two 1-ft.-long heat transfer sections, which allowed a wide variation in L/D. Heat transfer rates were measured by weighing the condensate collected over a timed interval. Heat balances, based upon the temperature rise and flow rate, were within an average of 7.7% of those based upon the condensate rate. Pressure taps were spaced at approximately 19-, 4¾-, 2¼-, and 2-ft. intervals. The wall temperature was measured with twelve to twenty-two thermocouples embedded in each diameter pipe. Flow rates were determined by diverting the fluid into a weigh tank for a timed interval.

The heat transfer instruments were calibrated individually where necessary. The adequacy of the equipment and procedures was checked by comparing experimental data on heating water with the Colburn (*11*) correlation; good agreement was obtained, as the standard deviation from the correlation was 3.2% for eight data points. Pressure loss-flow rate data were taken by Hanks (*20*) for water flowing in the apparatus, and good agreement with a standard friction factor correlation (39) is shown by the standard deviation of 4.0% for forty data points.

TRANSITIONAL FLOW CORRELATION

The mechanisms of flow and heat transfer change throughout the transition region, which is usually considered to be limited to the Reynolds number range of 2,100 to 10,000 for Newtonian flow. The use of a conventional correlation in the transition region, with dimensionless groups raised to exponential powers, is difficult due to the inconstancy of the exponents. The situation becomes much more complex when the dimensionless Reynolds number and Prandtl number must be defined for non-Newtonian fluids, which have viscosities varying not only with flow rate but with radial position in the pipe.

It will be demonstrated that these phenomena can be integrated into a transitional flow heat transfer correlation by means of a normalizing procedure, which accounts for the change of mechanism throughout the transition region. In this normalizing procedure, the following ratios are employed:

1. ϕ_j, the ratio at a given flow rate in the transition region, of the actual heat transfer rate to the heat transfer rate that would be obtained if the fully developed turbulent flow heat transfer mechanism existed.

2. ϕ_{jc}, the foregoing ratio taken at the critical flow rate, where the transition from laminar to turbulent flow begins.

The normalizing procedure is to divide the logarithm of ϕ_j by the logarithm of ϕ_{jc} to form a parameter which is postulated, subject to experimental proof, to be a function only of the ratio between the given flow rate U (at which ϕ_j is determined), and the critical flow rate U_c (at which ϕ_{jc} is determined):

$$\log \phi_j / \log \phi_{jc} = \text{function of } (U/U_c) \qquad (12)$$

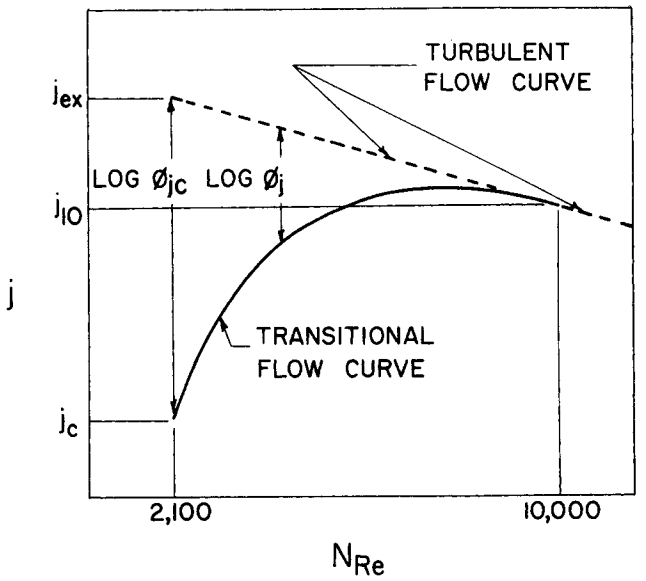

Fig. 2. Illustration of the deviation of the transitional flow heat transfer curve from the extrapolated turbulent flow line on a log-log plot and a graphical representation of log ϕ_j and log ϕ_{jc}.

The interpretation of log ϕ_j and log ϕ_{jc} follows from the proportionality between heat transfer rates and the corresponding j factors. The quantities log ϕ_j and log ϕ_{jc} are graphically illustrated in Figure 2 as linear distances of deviation of the transitional flow curve from the turbulent flow curve on a log-log plot of j vs. N_{Re}.

It is advantageous to relate the ratio log ϕ_j/log ϕ_{jc} to N_{Re} rather than to U/U_c; this is facilitated by defining N_{Re} as

$$N_{Re} \equiv 2{,}100\ (U/U_c) \qquad (13)$$

Equation (13) is readily related to the conventional Reynolds number

$$N_{Re} \equiv (DU\rho/\mu) \qquad (14)$$

Equation (14) is evaluated at the critical flow rate

$$2{,}100 \equiv (DU_c\rho/\mu) \qquad (15)$$

and Equation (15) is divided into Equation (14) to obtain Equation (13).

It follows from Equations (12) and (13) that the ratio log ϕ_j/log ϕ_{jc} is a function of N_{Re} as well as U/U_c, and the following definition is made:

$$\phi(Re) \equiv (\log \phi_j / \log \phi_{jc}) \qquad (16)$$

The $\phi(Re)$ function has the convenient boundary conditions of $\phi(Re) = 0$ at $N_{Re} = 10{,}000$, where the fully developed turbulent flow heat transfer mechanism exists, and $\phi(Re) = 1$ at $N_{Re} = 2{,}100$.

The equation of the turbulent flow heat transfer curve (the broken line in Figure 2) may be written

$$j = \psi(Re) \quad \text{(turbulent)} \qquad (17)$$

Newtonian Fluid Correlation

For Newtonian fluids, Equation (17) is nearly a straight line on a log-log plot of j vs. N_{Re}. With good accuracy, $\psi(Re)$ may be written as a function of the form

$$j = j_{10}\left(\frac{N_{Re}}{10{,}000}\right)^{\beta} \quad \text{(turbulent)} \qquad (18)$$

where β is the slope of the line on a log-log plot.

The equation of the transitional flow heat transfer curve is by definition given by ϕ_j times the turbulent flow j of

Equation (18):

$$j = j_{10}\left(\frac{N_{Re}}{10{,}000}\right)^{\beta}\phi_j \quad \text{(transitional)} \tag{19}$$

An expression for ϕ_j is obtained by rearranging Equation (16)

$$\phi_j = (\phi_{jc})^{\phi(Re)} \tag{20}$$

It may be seen from Figure 2 that

$$\phi_{jc} = (j_c/j_{ex}) \tag{21}$$

The value of j_{ex} is found by setting $N_{Re} = 2{,}100$ in Equation (18)

$$j_{ex} = j_{10}(2{,}100/10{,}000)^{\beta} \tag{22}$$

Substitution of Equations (20), (21), and (22) into (19) yields the transitional flow equation for heat transfer to Newtonian fluids:

$$j = j_{10}\left(\frac{j_c}{j_{10}}\right)^{\phi(Re)}\left(\frac{N_{Re}}{10{,}000}\right)^{\beta}\left(\frac{10{,}000}{2{,}100}\right)^{\beta\phi(Re)} \tag{23}$$

Equation (23) may be expressed in the equivalent form

$$N_{St} = (N_{St})_{10}\left[\frac{(N_{St})_c}{(N_{St})_{10}}\right]^{\phi(Re)}\left(\frac{N_{Re}}{10{,}000}\right)^{\beta}\left(\frac{10{,}000}{2{,}100}\right)^{\beta\phi(Re)} \tag{24}$$

since the factor $(N_{Pr})^{2/3}(\mu_w/\mu_b)^{0.10}$ cancels out of all of the j factors.

Determination of $\phi(Re)$

An expression for evaluating $\phi(Re)$ from experimental data is obtained by taking the log of Equation (24) and by rearranging

$$\phi(Re) = \frac{\log\left[\dfrac{(N_{St})}{(N_{St})_{10}}\left(\dfrac{10{,}000}{N_{Re}}\right)^{\beta}\right]}{\log\left[\dfrac{(N_{St})_c}{(N_{St})_{10}}\left(\dfrac{10{,}000}{2{,}100}\right)^{\beta}\right]} \tag{25}$$

To find the shape of the $\phi(Re)$ vs. N_{Re} curve, four sets of Newtonian flow heat transfer data with different L/D with the entire transition region well represented with data points in each set were chosen from the literature (*10, 17, 37, 48*). Values of $(N_{St})_c$ and $(N_{St})_{10}$, found by interpolation of experimental data, were used in Equation (25) to calculate $\phi(Re)$ for each (N_{St}, N_{Re}) data point. The slope β was determined from a log-log plot of the experimental turbulent flow values of j vs. N_{Re}. The computed values of $\phi(Re)$ are plotted in Figure 3.

The curve in Figure 3 is the plot of an empirical, analytical expression for $\phi(Re)$ in terms of N_{Re} derived from a function $f(Re)$, determined empirically by Kuznetsov and Leonencke (*30*). They proposed correlating transitional flow heat transfer data for Newtonian fluids by means of the equation

$$N_{Nu} = 0.021\,(N_{Re})_b^{0.8}\,(N_{Pr})_b^{0.43}\,(\mu_w/\mu_b)^{0.25} f(Re)\,(N_{Gr})^{X} \tag{26}$$

The equation

$$N_{Nu} = 0.021\,(N_{Re})_b^{0.8}\,(N_{Pr})_b^{0.43}\,(\mu_w/\mu_b)^{0.25} \tag{27}$$

was used for the turbulent flow region. Equation (26) was obtained by multiplying $f(Re)$ times the right side of Equation (27) to account for the effect of the varying transitional flow mechanism on heat transfer and by multiplying $(N_{Gr})^X$ times the right side of Equation (27) to account for the effect of free convection on heat transfer.

The $f(Re)$ function, which is identical to ϕ_j by definition, was found (*30*) at $N_{Gr} = 1$ and at a single unknown value of L/D to be given by the empirical equation

$$\phi_j \equiv f(Re) = 1.133\,\frac{(N_{Re} - 1{,}800)}{(N_{Re} - 710)} \tag{28}$$

The exponent X was determined (*30*) from data at various values of N_{Gr} to be given by

$$X = -0.167\,\log f(Re) \tag{29}$$

The result of Kuznetsov and Leonencke, Equation (28), is extended to the more general $\phi(Re)$ function by combining Equations (16) and (28) and by noting that ϕ_{jc} is determined at $N_{Re} = 2{,}100$.

$$\phi(Re) = \frac{\log\left[1.133\,\dfrac{(N_{Re} - 1{,}800)}{(N_{Re} - 710)}\right]}{\log\left[1.133\,\dfrac{(2{,}100 - 1{,}800)}{(2{,}100 - 710)}\right]} \tag{30}$$

Simplification of Equation (30) yields the empirical equation

$$\phi(Re) = 1.635\log\left[\frac{1}{1.133}\,\frac{(N_{Re} - 710)}{(N_{Re} - 1{,}800)}\right] \tag{31}$$

which is the equation plotted in Figure 3. It might be noted that $\phi(Re)$ is postulated to be independent of L/D, but the $f(Re)$ of Kuznetsov and Leonencke definitely is a function of L/D.

Discussion

The agreement of Equation (31) with the data in Figure 3 is very good; hence, Equation (31) may be used to compute $\phi(Re)$ for use in Equations (23) or (24). The postulate that $\phi(Re)$ is a function only of N_{Re} is supported at least over the L/D range of 118 to 197. A wider range of L/D is covered with the non-Newtonian fluid data in Figure 4. Although Equation (28) is restricted to a single value of L/D, it appears that the L/D

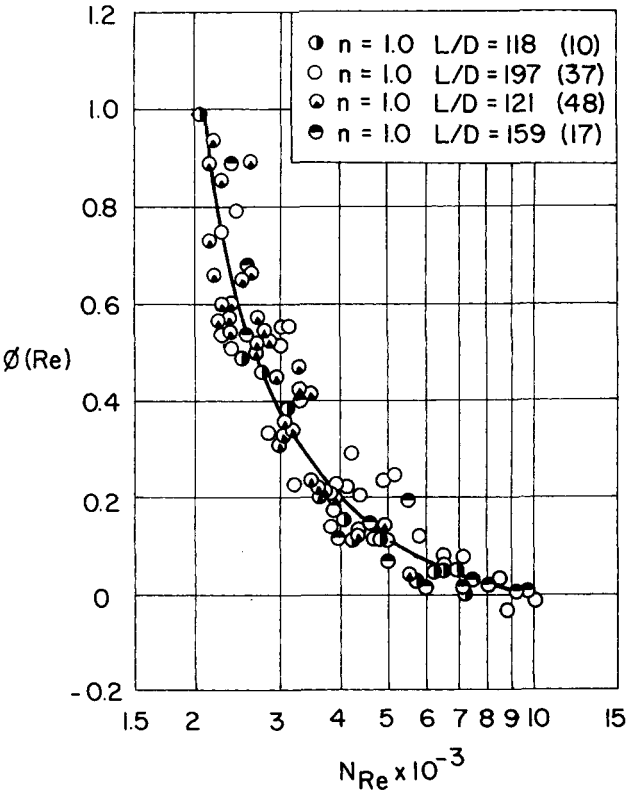

Fig. 3. A comparison of the $\phi(Re)$ function of Equation (31) with Newtonian fluid heat transfer data where $N_{Pr} > 2$.

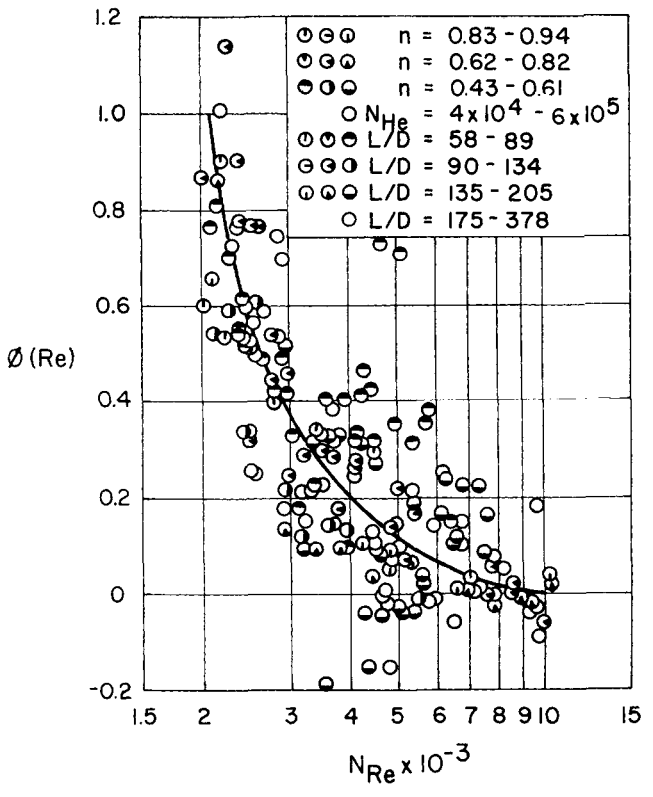

Fig. 4. A comparison of the $\phi(Re)$ function of Equation (31) with non-Newtonian fluid heat transfer data where $(N_{Pr})_{10} > 2$.

dependence is adequately cancelled by means of the $\phi(Re)$ ratio formulated from Equation (28) and given by Equation (31).

Some Newtonian fluid heat transfer data do not agree with the $\phi(Re)$ curve. Data for liquid metals (*2, 25*) apparently disagree with Equation (31) due to the very low Prandtl number. In the case of liquid metals, no discontinuity is observed in the heat transfer data at $N_{Re} = 2{,}100$, probably because heat transfer by molecular conduction is large compared to heat transfer by turbulence. Also, data for air (*6, 29*) are not in good agreement with Equation (31), because of the gradual transition to a turbulent flow heat transfer mechanism observed in the N_{Re} range of 2,100 to 5,000. Consequently, the correlation for $\phi(Re)$ is not considered applicable to gases or fluids with N_{Pr} less than about 2.

Non-Newtonian Fluid Correlation

The groups $(N_{St})_c$ and $(N_{St})_{10}$ in Equation (24) for Newtonian fluid heat transfer in transitional flow are constants for a given system, including non-Newtonian fluids. The N_{St} is a function of N_{Re} (and $\phi(Re)$) and β, which is a function of n, N_{Pr}, and N_{Re}. To utilize conveniently Equation (24) for non-Newtonian fluids, it will be assumed that β is a sufficiently weak function of N_{Re} in order to consider β independent of N_{Re}. Calculations have shown that the error in the assumption of β independent of N_{Re} is minimized if β is evaluated at $N_{Re} = 7{,}000$ and $(N_{Pr})_7$. The error does not exceed about 8% in N_{St} for n as low as 0.2. Therefore, the relation

$$\beta = \beta_7 = \text{function of } n, (N_{Pr})_7 \text{ and } (N_{Re})_7 \qquad (32)$$

will be used for non-Newtonian fluids.

The applicability of Equation (24) to non-Newtonian fluids will be tested with the data of Friend (*16, 36*), Haines (*19*), Raniere (*43*), and this work (*40*) on pseudoplastic fluids and of Thomas (*51, 52*) on approximate Bingham plastic fluids.

The quantities U_c, $(N_{Re})_{wc}$, $(N_{St})_c$, $(N_{St})_{10}$, and β_7 that are required to calculate N_{Re} and $\phi(Re)$ from Equations (13) and (25), respectively, could be found by interpolation or extrapolation of the experimental data as was done for the Newtonian fluid data presented in Figure 3. But the limited number of data points in some sets of data made this empirical determination unreliable. It was therefore decided to put the $\phi(Re)$ function to a stronger test and to calculate U_c, $(N_{Re})_{wc}$, $(N_{St})_c$, $(N_{St})_{10}$, and β_7 from the known fluid physical properties by empirical methods given in the sections on Calculation of Variables. However, experimental values of f_t were used, as they were available.

The $\phi(Re)$ data are plotted in Figure 4. A study of the data in Figure 4 shows no dependence of the $\phi(Re)$ function on L/D, n, or N_{He}. Consequently, $\phi(Re)$ is not a function of the geometry of the system or the type of fluid—Newtonian, pseudoplastic, or Bingham plastic. The $\phi(Re)$ function is evidently dependent only upon the N_{Re} defined by Equation (13).

In Figure 4, the data approach $\phi(Re) = 0$ as N_{Re} approaches 10,000, and the condition at which $\phi(Re) = 0$ is by definition the turbulent flow end of the transition region. The laminar flow limit of $\phi(Re) = 1$ as N_{Re} approaches 2,100 is similarly approached by the data. Therefore, a given numerical value of N_{Re} defined by Equation (13) has a similar meaning for Newtonian and non-Newtonian fluids, and a basic similarity in heat transfer mechanism at a given N_{Re} in the transition region is implied.

The apparently large scatter of the data in Figure 4 is a result of normal experimental error, and the errors in the calculation of U_c, $(N_{Re})_{wc}$, $(N_{St})_c$, $(N_{St})_{10}$, and β_7 quantities which are required to calculate $\phi(Re)$ and N_{Re}. With all the errors accumulated in the exponent $\phi(Re)$, the scatter appears large. However, it is significant that the scatter is random with respect to L/D, n, and N_{He}. Furthermore, the final test of the scatter is made best by comparison of experimental N_{St} or j factors with the corresponding quantities calculated from Equations (23) or (24) using the same data presented in Figure 4. This test is given in the section below where the experimental data are plotted on conventional j factor vs. N_{Re} coordinates. The j factor is arbitrarily defined for illustrative purposes as

$$j \equiv (N_{St})\ (N_{Pr})_{10}^{2/3}\ (\mu_{ww}/\mu_{wb})^{0.10} \qquad (33)$$

for pseudoplastic fluids and

$$j \equiv (N_{St})\ (N_{Pr})_{10}^{2/3}\ (\eta_w/\eta_b)^{0.10} \qquad (34)$$

for Bingham plastic fluids. The j factor definition does not have fundamental significance in the correlation, because all but the N_{St} factor cancel out of Equation (33) or (34) when used in the correlation, Equation (23).

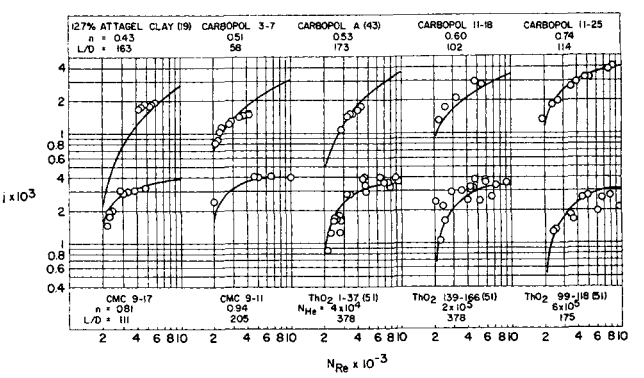

Fig. 5. Comparison of experimental data with the predictions of the equation for transitional flow heat transfer, Equation (23).

Final Test of the Non-Newtonian Correlation

Equation (23) represents a unique curve for each different non-Newtonian fluid on j factor vs. N_{Re} coordinates. The calculated curves are plotted in Figure 5 for one-half (to conserve space) of the fluids studied; the curves for the other fluids are given in reference *40*. Experimental data points are plotted for comparison with the curves. The standard deviation between all the experimental data and calculated curves is 17.7% and the average deviation is + 0.7% for one hundred and seventy data points. Since the standard deviation of 17.7% is reasonable for heat transfer data, particularly in the transition region, it is concluded that the scatter in the $\phi(Re)$ vs. N_{Re} plot is also reasonable. The small average deviation confirms that there is no bias in the correlation.

Discussion

The agreement between the data and the transitional flow heat transfer correlation is considered good. A wide range of variables was covered: $n = 0.43$ to 1.00 for pseudoplastic fluids, $N_{He} = 4 \times 10^4$ to 6×10^6 for Bingham plastic fluids, $D = 5/16$ to 2 in., $L/D = 58$ to 378, $(N_{Pr})_{10} = 7.5$ to 187, $N_{Re} = 2{,}100$ to 10,000, and $(\mu_{ww}/\mu_{wb})^{0.10} = 0.90$ to 1.00.

The $\phi(Re)$ function, with a properly defined Reynolds number, has been shown to account for the effect of change of heat transfer mechanism in transitional flow. The $\phi(Re)$ function is evidently independent of L/D at least for $L/D > 60$, of non-Newtonian properties for pseudoplastic and Bingham plastic fluids, and of $(N_{Pr})_{10}$ for $(N_{Pr})_{10} > 2$.

The success of the $\phi(Re)$ function implies a basic similarity in transitional flow heat transfer mechanisms between Newtonian and non-Newtonian fluids. The most important corollaries of the proven $\phi(Re)$ function are:

1. A Reynolds number *linear* in flow rate is unexpectedly required to correlate transitional flow heat transfer data for non-Newtonian fluids.
2. The transition from laminar to fully developed turbulent flow extends over the *same* range of flow rates for both Newtonian and non-Newtonian fluids.
3. A given value of Reynolds number in the range of 2,100 to 10,000 has the same significance in regard to transitional flow heat transfer mechanisms whether the fluid is Newtonian or non-Newtonian.

CALCULATION OF VARIABLES—PSEUDOPLASTIC FLUIDS

In order to use the previously developed correlations for turbulent or for transitional flow to predict heat transfer rates, one must calculate pertinent variables from the properties of non-Newtonian fluids. Equations are derived below to calculate these variables.

The rheological data for pseudoplastic fluids are commonly given as a log-log plot of τ_w vs. $\dot{S}_w$ from a rotary viscometer or of τ_w vs. (4Γ) from a capillary viscometer. If n and K are constants, Equation (1) may be integrated to obtain

$$\tau_w = K\left(\frac{3n+1}{4n}\right)^n (4\Gamma)^n \tag{35}$$

Comparison of Equation (35) with (1) at $\tau = \tau_w$ and $\dot{S} = \dot{S}_w$ leads to

$$\dot{S}_w = \left(\frac{3n+1}{4n}\right)(4\Gamma) \tag{36}$$

which was also developed by Rabinowitsch (*42*). Equation (36) readily allows τ_w vs. $\dot{S}_w$ data to be expressed as τ_w vs. (4Γ).

A common alternate way to express Equation (1) is

$$\tau_w = K'(4\Gamma)^{n'} \tag{37}$$

Comparison of Equation (37) with (35) yields

$$K' = K\left(\frac{3n+1}{4n}\right)^n \tag{38}$$

and

$$n' = n \tag{39}$$

where n and K are independent of τ_w.

The effect of temperature on rheological data may be determined (*11*) from the definition

$$\frac{\Delta H^{\ddagger}}{R} \equiv -\left[\frac{\partial \ln \dot{S}}{\partial (1/T)}\right]_{\tau = \text{const.}} \tag{40}$$

The $\Delta H^{\ddagger}/R$ is evaluated at constant τ_w at two temperatures from finite differences of Equation (40):

$$\frac{\Delta H^{\ddagger}}{R} = \left(\frac{T_1 T_2}{T_2 - T_1}\right)\ln\left(\frac{\dot{S}_2}{\dot{S}_1}\right) \tag{41}$$

From Equation (41) and the definition of viscosity the correction factor is obtained:

$$\left(\frac{\mu_{ww}}{\mu_{wb}}\right)^{-0.10} = e^{0.10\,\frac{\Delta H^{\ddagger}}{R}\,\frac{(T_w - T_b)}{T_w T_b}} \tag{42}$$

U_c, τ_{wc}, $(N_{Re})_{wc}$, and $(N_{Pr})_c$

The critical flow rate for pseudoplastic fluids may be obtained from the theory of Ryan and Johnson (*26, 45*) as generalized by Hanks (22, 23). The theory states that the maximum value (at the radius of least stable flow) of the stability parameter

$$Z' = \frac{1}{2}\,\frac{\rho}{(dp/dz)}\left(-\frac{du}{dr}\right) \tag{43}$$

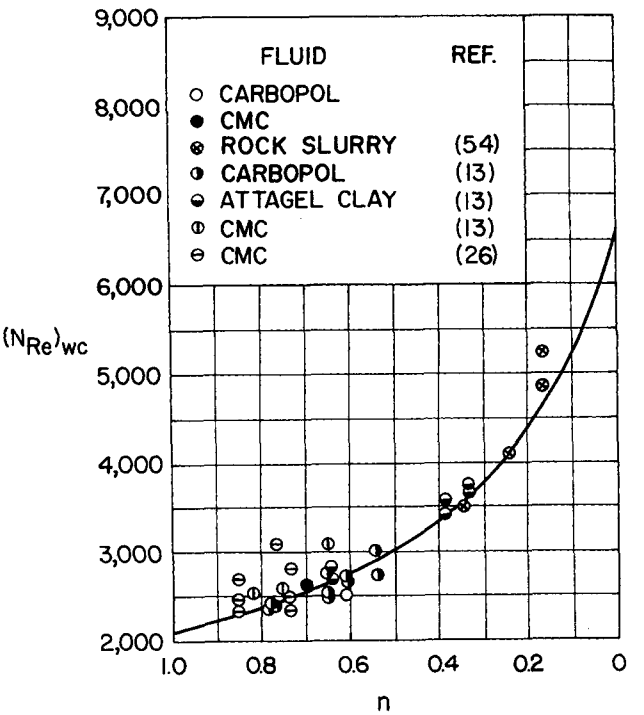

Fig. 6. Comparison of experimental data for $(N_{Re})_{wc}$ with a plot of Equation (51).

should be the same at the critical flow rate for pseudoplastic fluids as it is for Newtonian fluids:

$$Z'_m = 404 \tag{44}$$

Equation (43) may be evaluated at the maximum value of Z' by the condition that $(dZ'/dr) = 0$. The result for pseudoplastic fluids that follow Equation (1) is (*26*)

$$\tau_{wc} = \frac{\rho D^2(4\Gamma_c)^2}{128 g_c Z'_m} \frac{(3n+1)^2}{n} \left(\frac{1}{n+2}\right)^{\frac{n+2}{n+1}} \tag{45}$$

Equation (45) may also be written (*20*) in the form

$$f_{fc} = \frac{1}{Z'_m} \frac{(3n+1)^2}{n} \left(\frac{1}{n+2}\right)^{\frac{n+2}{n+1}} \tag{46}$$

by means of Equations (48) and (62).

The critical velocity U_c may be obtained by substitution of τ_{wc} from Equation (35) evaluated at the critical flow rate into Equation (45):

$$U_c = \frac{n}{(3n+1)} \left\{ \frac{2^{n+1} g_c K Z'_m}{\rho D^n} \frac{(n+2)^{\frac{n+2}{n+1}}}{n} \right\}^{\frac{1}{2-n}} \tag{47}$$

The value of

$$U_c = \frac{D(4\Gamma_c)}{8} \tag{48}$$

may also be obtained as the intersection of Equation (45) with a log τ_w vs. log (4Γ) plot of tube viscometer data.

The expression for $(N_{Re})_{wc}$ is obtained from the definitions

$$(N_{Re})_{wc} \equiv (DU_c \rho/\mu_{wc}) \tag{49}$$

and

$$\mu_{wc} \equiv (g_c \tau_{wc}/\dot{S}_{wc}) \tag{50}$$

and from Equations (1), (35), and (45); the result is

$$(N_{Re})_{wc} = 4Z'_m \frac{(n+2)^{\frac{n+2}{n+1}}}{(3n+1)} \tag{51}$$

Equation (51) is plotted as the solid line in Figure 6, and data points are given for comparison.

The value of $(N_{Pr})_c$ is readily obtained from the definition

$$(N_{Pr})_c \equiv (C_p \mu_{wc}/k)\ [(N_{Re})_{wc}/2{,}100] \tag{52}$$

$(N_{St})_c$, $(N_{Gz})_c$, ϕ_{nT}, and (L/D)

The Stanton number at the critical flow rate may be obtained from a laminar flow correlation for heat transfer. The preferred laminar flow correlation is given by Christiansen and Craig (*7*). The correlation accounts for the effects of temperature profile and pseudoplastic fluid properties upon the heat transfer rate. It was found (*7*) that two parameters, $\psi(H) \equiv \Delta H^{\neq}/R(1/T_{in} - 1/T_w)$ and n, were required on a log-log plot of N_{Nu} vs. N_{Gz}. For convenience, the correlation of Christiansen and Craig for heating is replotted in Figure 7 with ϕ_{nT} in place of N_{Nu}. Data for computation of the ϕ_{nT} for cooling, where $\psi(H)$ is negative, are available for power law fluids (*50*). The factor ϕ_{nT} is the multiplier required in the simple Levêque (*31*) equation to make it agree with the correlation of Christiansen and Craig. The modified equation obtained with the ϕ_{nT} multiplier is

$$\left(\frac{h}{C_p G}\right)\left(\frac{C_p \mu}{k}\right)^{2/3} = 1.75\left(\frac{L}{D}\right)^{-1/3}\left(\frac{DU\rho}{\mu}\right)^{-2/3} \phi_{nT} \tag{53}$$

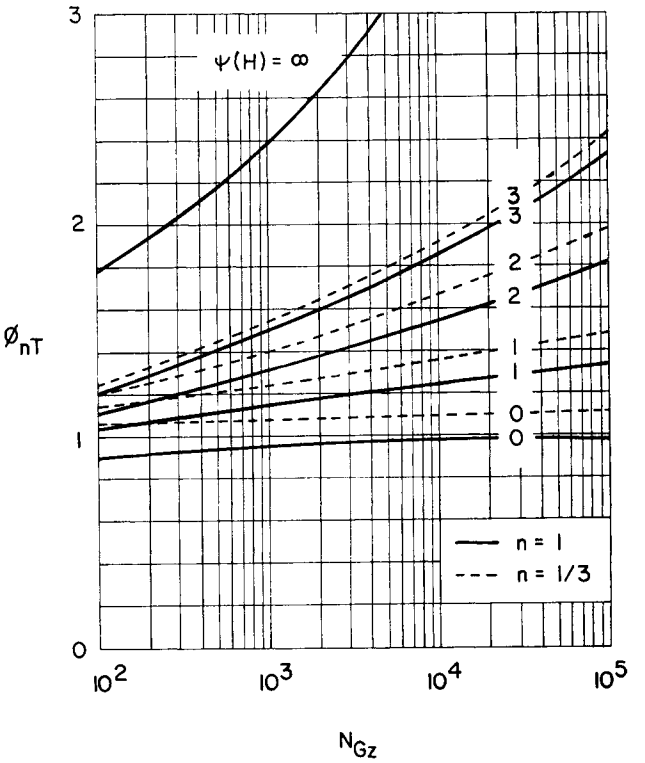

Fig. 7. Plot of the ϕ_{nT} factor of Equation (54) for laminar flow heat transfer.

Evaluation of μ in Equation (53) at the wall and critical flow rate conditions followed with the substitution of Equation (52), yields

$$(N_{St})_c = \frac{0.0106\ \phi_{nT}}{(L/D)^{1/3}\ (N_{Pr})_c^{2/3}} \tag{54}$$

The critical Graetz number is obtained from the definition

$$(N_{Gz})_c \equiv \frac{\pi D \rho C_p U_c}{4k\ (L/D)} \tag{55}$$

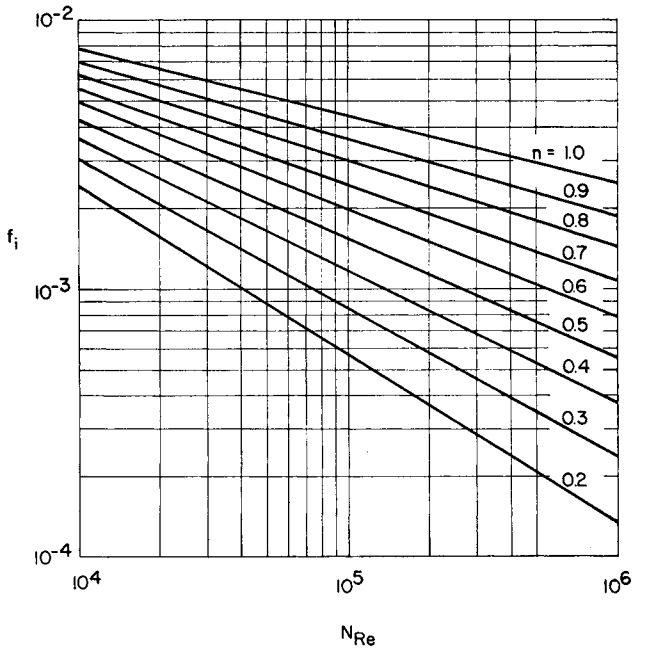

Fig. 8. Plot of f_i for turbulent flow.

A value of (L/D) must often be assumed for use in Equations (54) and (55). The assumed value may be checked from the calculated value of U_o by the expression

$$L/D = \frac{\rho C_p U_c (t_2 - t_1)}{4U_o\,\Delta t_o}\left(\frac{N_{Re}}{2{,}100}\right) \tag{56}$$

derived from the familiar equations

$$q = U_o A\,\Delta t_o \tag{57}$$

and

$$q = W\,C_p(t_2 - t_1) \tag{58}$$

f_{i10}, τ_{w10}, and $(N_{Pr})_{10}$

Friction factor data for non-Newtonian fluids in turbulent flow were correlated by Dodge (*13, 14*) with the equation

$$f_i = a_n\left(\frac{D^{n'}U^{2-n'}\rho}{8^{n'-1}g_c K'}\right)^{-b_n} \tag{59}$$

Substitution of Equations (13), (38), and (39) into (59) yields

$$f_i = a_n\left[\frac{D^n U_c^{2-n}\rho}{8^{n-1}g_c K}\left(\frac{N_{Re}}{2{,}100}\right)^{2-n}\left(\frac{4n}{3n+1}\right)^n\right]^{-b_n} \tag{60}$$

Substitution of Equation (47) into (60) yields

$$f_i = a_n\left[Z'_m\left(\frac{4n}{3n+1}\right)^2\frac{(n+2)^{\frac{n+2}{n+1}}}{n}\right]^{-b_n}\left(\frac{N_{Re}}{2{,}100}\right)^{-(2-n)b_n} \tag{61}$$

A plot of f_i is given in Figure 8, where f_{i10} is the value of f_i at $N_{Re} = 10{,}000$. The a_n and b_n functions were given by Dodge (*13, 14*).

The definition of friction factor is

$$\tau_w \equiv \frac{f_i \rho U^2}{2g_c} \tag{62}$$

To obtain τ_w at any N_{Re}, Equation (13) is substituted into Equation (62):

$$\tau_w = \frac{f_i \rho U_c^2}{2g_c}\left(\frac{N_{Re}}{2{,}100}\right)^2 \tag{63}$$

The quantity τ_{w10} is found from Equation (63) evaluated at f_{i10} and $N_{Re} = 10{,}000$.

The quantity $(N_{Pr})_{10}$ is found from the definition

$$(N_{Pr})_{10} \equiv (C_p\mu_{w10}/k)\,[(N_{Re})_{wc}/2{,}100] \tag{64}$$

where

$$\mu_{w10} \equiv g_c\,\tau_{w10}/\dot{S}_{w10} \tag{65}$$

The value of $\dot{S}_{w10}$ is obtained from viscometer data at τ_{w10} and at t_b.

An alternate equation for calculating $(N_{Pr})_{10}$ is derived below for n = constant. The ratio of τ_w is obtained from Equation (63):

$$\frac{\tau_w}{\tau_{wc}} = \frac{f_i}{f_{ic}}\left(\frac{N_{Re}}{2{,}100}\right)^2 \tag{66}$$

The ratio of $\dot{S}_w$ is obtained from Equation (1):

$$\frac{\dot{S}_{wc}}{\dot{S}_w} = \left(\frac{\tau_{wc}}{\tau_w}\right)^n \tag{67}$$

From the definition of N_{Pr}

$$\frac{N_{Pr}}{(N_{Pr})_c} = \frac{\tau_w}{\dot{S}_w}\cdot\frac{\dot{S}_{wc}}{\tau_{wc}} \tag{68}$$

Substitution of Equations (66) and (67) into (68) yields

$$N_{Pr} = (N_{Pr})_c\left[\frac{f_{ic}}{f_i}\left(\frac{2{,}100}{N_{Re}}\right)^2\right]^{\frac{1-n}{n}} \tag{69}$$

At $N_{Re} = 10{,}000$

$$\frac{(N_{Pr})_c}{(N_{Pr})_{10}} = \left[\frac{f_{i10}}{f_{ic}}\left(\frac{10{,}000}{2{,}100}\right)^2\right]^{\frac{1-n}{n}} \tag{70}$$

The right side of Equation (70) is a function of n only. The f_{ic} is calculated from Equation (46) and the f_{i10} is taken from Figure 8.

$(N_{St})_{10}$, β_7, ϕ_m, and θ_m

The quantity $(N_{St})_{10}$ is calculated from Equation (9) evaluated at $N_{Re} = 10{,}000$:

$$(N_{St})_{10} = \frac{\left(\frac{f_{i10}}{2\theta_m}\right)\left(\frac{\mu_{ww}}{\mu_{wb}}\right)^{-0.10}}{\frac{1}{\phi_m} + 11.8\sqrt{\frac{f_{i10}}{2}}\,\frac{[(N_{Pr})_{10}-1]}{(N_{Pr})_{10}^{1/3}}} \tag{71}$$

An expression for β_7 may be found by evaluating

$$\beta = (d\log j/d\log N_{Re}) \tag{72}$$

at $N_{Re} = 7{,}000$. Equations (9) and (33) are substituted into Equation (72), and the derivative is taken to yield an expression containing (df_i/dN_{Re}) and (dN_{Pr}/dN_{Re}). The derivative

$$\left(\frac{df_i}{dN_{Re}}\right) = \frac{f_i}{N_{Re}}(n-2)b_n \tag{73}$$

is found from Equation (61). The derivative

$$\left(\frac{dN_{Pr}}{dN_{Re}}\right) = \frac{N_{Pr}}{N_{Re}}\left(\frac{n-1}{n}\right)[(n-2)\,b_n + 2] \tag{74}$$

is found from Equations (7), (8), (47), and (63).

When (df_i/dN_{Re}) and (dN_{Pr}/dN_{Re}) are eliminated by means of Equations (73) and (74), and the condition of $N_{Re} = 7{,}000$ is imposed, the expression for β_7 becomes

$$\beta_7 = \left.\frac{(n-2)b_n\left[\frac{1}{\phi_m} + \frac{11.8}{2}\sqrt{\frac{f_i}{2}}\,\frac{(N_{Pr}-1)}{N_{Pr}^{1/3}}\right] + \frac{11.8}{3}\sqrt{\frac{f_i}{2}}\left(\frac{1-n}{n}\right)[(n-2)b_n+2]\left[\frac{2N_{Pr}+1}{N_{Pr}^{1/3}}\right]}{\left[\frac{1}{\phi_m} + 11.8\sqrt{\frac{f_i}{2}}\,\frac{(N_{Pr}-1)}{N_{Pr}^{1/3}}\right]}\right|_{N_{Re}=7{,}000} \tag{75}$$

For convenience in calculations, β_7 is plotted in Figure 9.

The ϕ_m factor is based upon the correlation of Dodge and Metzner (*14*) for velocity distribution.

$$u_m - u = -5.660\,n^{0.25}\sqrt{\frac{g_c\tau_w}{\rho}}\log\frac{R-r}{R} \tag{76}$$

From Equation (76), it may be shown that

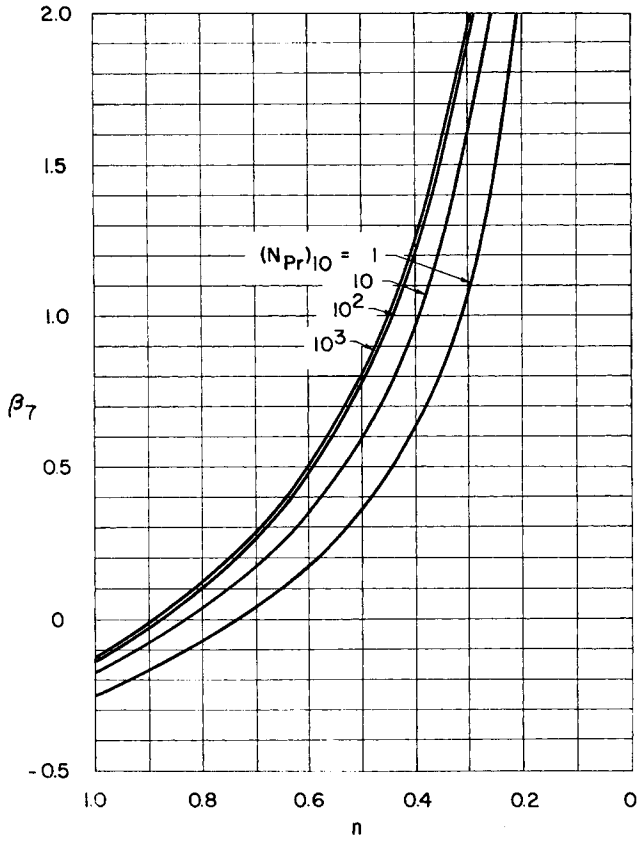

Fig. 9. Plot of β_7 for transitional flow heat transfer.

$$\phi_m \cong \frac{1}{1 + 3.68n^{0.25}\sqrt{f_i/2}} \tag{77}$$

The ϕ_m factor is tabulated in Table 1.

The θ_m factor is obtained from the calculations of Reichardt (*44*) for Newtonian fluids and is listed in Table 2. The extension of θ_m to non-Newtonian fluids is made approximately by the use of Equation (13) for the Reynolds number and Equation (8) for the Prandtl number.

CALCULATION OF VARIABLES—BINGHAM PLASTIC FLUIDS

The rheological constants η and τ_y may be evaluated from Equation (2) for rotary viscometer data or from the integrated form of Equation (2) for capillary viscometer data:

$$\tau_w = \tau_y\left[\frac{4}{3} - \frac{1}{3}\left(\frac{\tau_y}{\tau_w}\right)^3\right] + \frac{\eta}{g_c}(4\Gamma) \tag{78}$$

The slope on linear coordinates of the τ_w vs. $\dot{S}_w$ curve is η/g_c and the intercept at $\dot{S}_w = 0$ is τ_y. At large values of τ_w, where $(\tau_y/\tau_w)^3 << 4$, the slope on linear coordinates of the τ_w vs. (4Γ) curve is η/g_c and the tangent extrapolated to $(4\Gamma) = 0$ intercepts at $4\tau_y/3$.

U_c, $(N_{Re})_{\eta c}$, and $(N_{Pr})_c$

The prediction of the critical Reynolds number by the stability criterion of Equation (43) for fluid behavior described by Equation (2) may be shown to be given by the simultaneous solution of the equations.

$$(N_{Re})_{\eta c} = 3\sqrt{3}\ Z'_m \frac{\left(1 - \frac{4}{3}\alpha_c + \frac{1}{3}\alpha_c^4\right)}{(1-\alpha_c)^3} \tag{79}$$

Table 1. ϕ_m Factor

n	1.0	0.8	0.6	0.4	0.2
N_{Re}					
1×10^4	0.81	0.84	0.86	0.89	0.92
3×10^4	0.83	0.86	0.88	0.91	0.94
1×10^5	0.85	0.88	0.91	0.93	0.96
3×10^5	0.87	0.90	0.92	0.95	0.97

Table 2. θ_m Factor

N_{Pr}	1	3	10	30	100
N_{Re}					
10^4	0.84	0.90	0.95	0.97	0.99
10^5	0.86	0.91	0.95	0.98	0.99
10^6	0.88	0.92	0.95	0.98	0.99

and

$$\frac{\alpha_c}{(1-\alpha_c)^3} = \frac{N_{He}}{24\sqrt{3}\ Z'_m} \tag{80}$$

A plot of the solution of Equations (79) and (80) is shown in Figure 10 in comparison to experimental data points. Agreement between theory and experimental data at high N_{He} is not good. But an empirical curve is drawn through the data points to have an approximate means to predict $(N_{Re})_{\eta c}$ as a function of N_{He}.

The reason for the lack of agreement at high values of N_{He} is that the simple Equation (2) does not accurately represent the rheological data (*4, 8, 23*) of real fluids. If an accurate value of $(N_{Re})_{\eta c}$ is required, either a graphical procedure must be used (*4*) or a better rheological equation, such as the Powell-Eyring equation (*46*), must be used (*23*).

The critical velocity is given from the definition of $(N_{Re})_{\eta c}$.

$$U_c = (N_{Re})_{\eta c}\,\eta_b/D\rho \tag{81}$$

where $(N_{Re})_{\eta c}$ is evaluated from Figure 10.

For convenience, $(N_{Pr})_c$ will be arbitrarily defined as

$$(N_{Pr})_c \equiv (C_p\,\eta_b/k)\ [(N_{Re})_{\eta c}/2{,}100] \tag{82}$$

$(N_{St})_c$ and ϕ_{HeT}

The analog of Equation (53) for Bingham plastic fluids is

$$\left(\frac{h}{C_pG}\right)\left(\frac{C_p\eta}{k}\right)^{2/3} = 1.75\left(\frac{L}{D}\right)^{-1/3}\left(\frac{DU\rho}{\eta}\right)^{-2/3}\phi_{HeT} \tag{83}$$

By substituting $(N_{Pr})_c$ from Equation (82) into Equation (83), one obtains

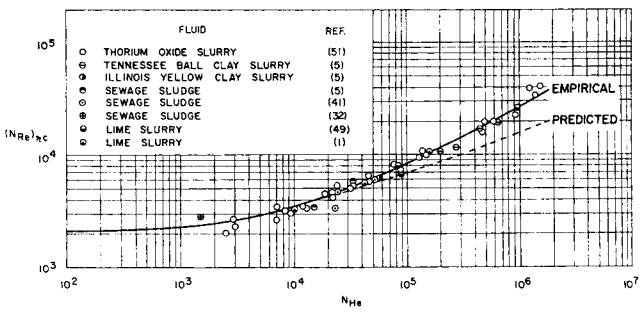

Fig. 10. Comparison of experimental data, the empirical curve, and the solution of Equations (79) and (80) for $(N_{Re})_{\eta c}$.

$$(N_{St})_e = \frac{0.0106\,\phi_{HeT}}{\left(\frac{L}{D}\right)^{1/3}\,(N_{Pr})_e^{2/3}} \qquad (84)$$

The factor ϕ_{HeT} is given in Figure 11 as a function of τ_y/τ_w, based upon the heat transfer calculations of Jensen (*24*) for the Bingham plastic model. At the critical flow rate, $\tau_y/\tau_w = 0.5$ corresponds to $N_{He} = 8 \times 10^4$ and $\tau_y/\tau_w = 0.7$ corresponds to $N_{He} = 6 \times 10^5$. The reciprocal of the ϕ_{HeT} obtained for the positive value of the same numerical $\psi(H)$ may be taken as an approximation for ϕ_{HeT} for cooling.

f_{i10} and $(N_{Pr})_{10}$

Friction factors for Bingham plastic fluids may be found by the empirical method of Thomas (*52*) used on thorium oxide suspensions. Transitional and turbulent flow friction factors were correlated with the Blasius (*27*) relationship.

$$f_i = B_1\,[DU\rho/\eta_b]^{-b} \qquad (85)$$

where the constants are given by the expressions

$$B_1 = 0.079\,(\mu_a/\eta)^{0.48} \qquad (86)$$

and

$$b = 0.25\,(\mu_a/\eta)^{0.15} \qquad (87)$$

Equation (85) is also conveniently written as

$$f_i = B_1\left[\,N_{Re}\,\frac{(N_{Re})_{\eta_0}}{2{,}100}\,\right]^{-b} \qquad (88)$$

The factor f_{i10} is found by evaluation of Equation (88) at $N_{Re} = 10{,}000$.

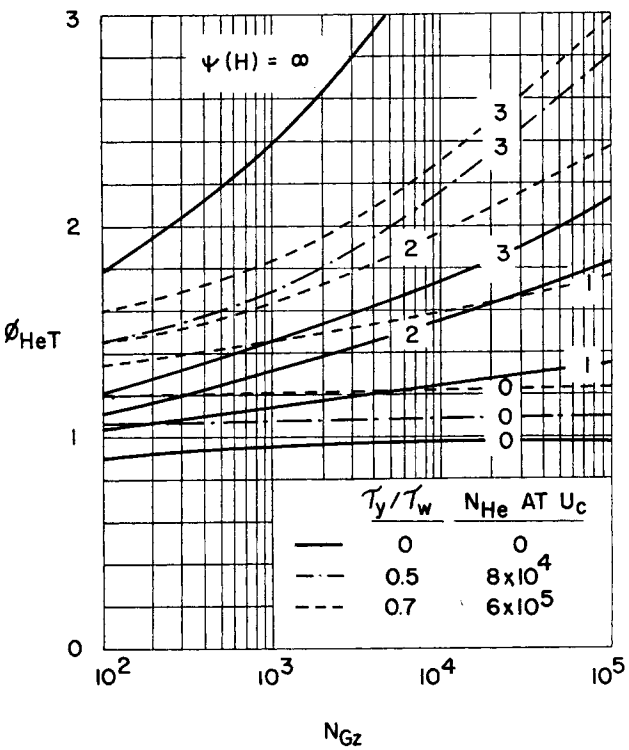

Fig. 11. Plot of the ϕ_{HeT} factor of Equation (83) for laminar flow heat transfer.

$$f_{i10} = B_1\left[\,\frac{10{,}000\,(N_{Re})_{\eta_0}}{2{,}100}\,\right]^{-b} \qquad (89)$$

The value of $(N_{Pr})_{10}$ is found by evaluation of Equation (11) at $N_{Re} = 10{,}000$:

$$(N_{Pr})_{10} = (N_{Pr})_{\eta_b} \qquad (90)$$

$(N_{St})_{10}$, β, ϕ_m and θ_m

The quantity $(N_{St})_{10}$ is calculated from Equation (10) evaluated at $N_{Re} = 10{,}000$:

$$(N_{St})_{10} = \frac{\left(\frac{f_{i10}}{2\theta_m}\right)\left(\frac{\eta_w}{\eta_b}\right)^{-0.10}}{\frac{1}{\phi_m} + 11.8\sqrt{\frac{f_{i10}}{2}}\,\frac{[(N_{Pr})_{10}-1]}{(N_{Pr})_{10}^{1/3}}} \qquad (91)$$

The exponent β is taken from Figure 10 at $n = 1.0$, since a Bingham plastic fluid is almost Newtonian at $N_{Re} = 10{,}000$.

The ϕ_m factor is taken from Table 1 at $n = 1.0$. The θ_m factor is given in Table 2.

SUMMARY

The correlations now available for predicting heat transfer rates to pseudoplastic and Bingham plastic non-Newtonian fluids in circular pipes and their limitations are:

Type of flow	N_{Re} range	Restrictions	Equations	Typical standard deviations
Laminar	<2,100	Free convecton negligible	(53) or (83)	—
Transitional	2,100 to 10,000	$(N_{Pr})_{10} > 2$	(23) or (24)	17.7%
Turbulent	>10,000	$N_{Re}(N_{Pr})_{10} > 2{,}500$	(9) or (10)	14.8%

The heat transfer correlations require only known data: the physical properties of the fluid including rheological data, and the geometrical constants of the system. All other data used in the correlation may be calculated from theory or from empirical equations as presented in the sections on Calculation of Variables. Several graphs and tables are included for more rapid evaluation of some variables. For assistance in numerical use of the methods suggested in this paper, a sample calculation for a practical problem is available.*

ACKNOWLEDGMENT

This paper is based on a doctoral thesis submitted to the University of Utah by A. W. Petersen.

The authors are grateful to the University of Utah Research Fellowship Fund and the Union Carbide Nuclear Company for financial support of this work and to the Hercules Powder Company for the carboxymethylcellulose used in experimentation.

NOTATION

A = surface area, sq. ft.
b = exponent defined by Equation (87), dimensionless
B_1 = exponent defined by Equation (86), dimensionless
C_p = heat capacity at t_b, B.t.u./(lb.)(°F.)
D = pipe diameter, ft.
f = Fanning friction factor, $(2g_c\,\tau_w/\rho U^2)$
$f(Re)$ = function defined by Equation (28), dimensionless

* Deposited as document 8651 with the American Documentation Institute, Photoduplication Service, Library of Congress, Washington 25, D. C., and may be obtained for $1.25 for photoprints or 35-mm. microfilm.

g_c = conversion factor, 32.17 $(\text{lb.}_m)(\text{ft.})/(\text{lb.}_f)(\text{sec.}^2)$
G = mass flow rate, lb./(sec.)(sq. ft.)
h = heat transfer coefficient, B.t.u./(sec.)(sq. ft.)(°F.)
j = j factor, $(N_{St})(N_{Pr})_{10}^{2/3}(\mu_{ww}/\mu_{wb})^{0.10}$, $(N_{St})(N_{Pr})_{10}^{2/3}(\eta_w/\eta_b)^{0.10}$, or $(N_{St})(N_{Pr})^{2/3}(\mu_w/\mu_b)^{0.10}$
k = thermal conductivity at t_b, B.t.u./(sec.)(ft.)(°F.)
K = consistency index, (lb.)(sec.^{n})/(sq. ft.)
K' = consistency index, (lb.)(sec.^{n})/(sq. ft.)
L = pipe length, ft.
n = flow behavior index, dimensionless
n' = flow behavior index, dimensionless
N_{Gz} = Graetz number, (wC_p/kL)
N_{Gr} = Grashof number, $(D^3\rho^2 g\beta\Delta t/\mu^2)$
N_{He} = Hedstrom number, $(\rho D^2\tau_y/g_c\mu^2)$
N_{Nu} = Nusselt number, (hD/k)
N_{Pr} = Prandtl number, $(C_p\mu/k)$, $(C_p\mu_{wb}/k)$ $[(N_{Re})_{wc}/2100]$ or $(C_p\eta_b/k)$
$(N_{Pr})_{wb}$ = Prandtl number, $(C_p\mu_{wb}/k)$
$(N_{Pr})_{\eta b}$ = Prandtl number, $(C_p\eta_b/k)$
N_{Re} = Reynolds number, 2,100 (U/U_c) or $(DU\rho/\mu_b)$
$(N_{Re})_{wc}$ = critical Reynolds number, $(DU\rho/\mu_{wb})_c$
$(N_{Re})_{\eta c}$ = critical Reynolds number, $(DU\rho/\eta_b)_c$
N_{St} = Stanton number, (h/C_pG)
p = pressure, lb./sq. ft.
q = heat transfer rate, B.t.u./sec.
Q = volumetric flow rate, cu. ft./sec.
r = radial distance, ft.
R = pipe radius, ft.
S = shear rate $-(du/dr)$, sec.$^{-1}$
t = temperature, °F.
T = absolute temperature, °R.
u = point velocity, ft./sec.
U = mean velocity, ft./sec.
U_o = overall heat transfer coefficient, B.t.u./(sec.)(sq. ft.)(°F.)
w = weight flow rate, lb./sec.
X = exponent defined by Equation (29), dimensionless
z = axial distance along pipe, ft.
Z' = stability parameter defined by Equation (43), dimensionless

Greek Letters

α = ratio, (τ_y/τ_w), dimensionless
β = slope of the turbulent flow heat transfer curve
Γ = flow function, $(Q/\pi R_w^3)$, sec.$^{-1}$
$\Delta H^{\ddagger}/R$ = constant defined by Equation (40), °R.$^{-1}$
Δt_o = overall temperature difference, °F.
η = coefficient of rigidity, lb./(sec.)(ft.)
θ_m = ratio of mean to maximum temperature difference
μ = viscosity, lb./(sec.)(ft.)
ρ = density at t_b, lb./cu. ft.
τ = shear stress, lb./sq. ft.
ϕ_j = ratio, at a given flow rate in the transition region, of the actual heat transfer rate to the heat transfer rate that would be obtained if the fully developed turbulent flow heat transfer mechanism existed
ϕ_{jc} = value of ϕ_j at critical flow rate $(N_{Re} = 2{,}100)$
ϕ_m = ratio of mean to maximum velocity, (U/u_m)
ϕ_{HeT} = laminar flow heat transfer correction factor for Bingham plastics, dimensionless
ϕ_{nT} = laminar flow heat transfer correction factor for pseudoplastics, dimensionless
$\phi(Re)$ = function of Reynolds number, $(\log\phi_j/\log\phi_{jc})$, dimensionless
$\psi(H)$ = laminar flow parameter, $\Delta H^{\ddagger}/R(1/T_{in} - 1/T_w)$, dimensionless
$\psi(Re)$ = turbulent flow heat transfer function, dimensionless

Subscripts

b = at the bulk fluid temperature
c = at the critical flow rate
e = effective
em = empirical
ex = turbulent flow function extrapolated to conditions at the critical flow rate
i = evaluated as if flow were isothermal at the bulk fluid temperature
in = inlet
$i10$ = evaluated as if flow were isothermal at the bulk fluid temperature and $N_{Re} = 10{,}000$
m = maximum
ni = nonisothermal
pr = predicted
s = suspending medium for a slurry
w = at the wall temperature or wall shear stress
wb = at the wall shear stress and bulk fluid temperature
wc = at the wall shear stress and critical flow rate
ww = at the wall shear stress and wall temperature
$w10$ = at the wall shear stress and $N_{Re} = 10{,}000$
y = yield
1 = at temperature 1
2 = at temperature 2
7 = evaluated at $N_{Re} = 7{,}000$
10 = evaluated at $N_{Re} = 10{,}000$
ηb = for a Bingham plastic fluid at the bulk fluid temperature
ηc = for a Bingham plastic fluid at the critical flow rate

LITERATURE CITED

1. Alves, G. E., D. F. Boucher, and R. L. Pigford, *Chem. Eng. Progr.*, **48**, 385 (1952).
2. Bailey, D. L. R., W. F. Cope, and G. G. Watson, *Natl. Phys. Lab. Eng. Div. N.O., 379/48* (1949).
3. Bonilla, C. F., A. Cervi, Jr., T. J. Colven, Jr., and S. J. Wang, *Chem. Eng. Progr. Symposium Ser. No. 5*, **49**, 127 (1953).
4. Brodkey, R. S., private communication (1963).
5. Caldwell, D. H., and H. E. Babbitt, *Ind. Eng. Chem.*, **33**, 249 (1941).
6. Cholette, A., *Chem. Eng. Progr.*, **44**, 81 (1948).
7. Christiansen, E. B., and S. E. Craig, Jr., *A.I.Ch.E. J.*, **8**, 154 (1962).
8. Christiansen, E. B., N. W. Ryan, and W. E. Stevens, *ibid.*, **1**, 544 (1955).
9. Chu, J. C., F. Brown, and K. G. Burridge, *Ind. Eng. Chem.*, **45**, 1686 (1953).
10. Clapp, M. H., and O. FitzSimons, S.M. thesis, Massachusetts Inst. Tech., Cambridge (1928).
11. Colburn, A. P., *Trans. Am. Inst. Chem. Engrs.*, **29**, 174 (1933).
12. Craig, S. E., Jr., Ph.D. thesis, Univ. Utah, Salt Lake City (1959).
13. Dodge, D. W., Ph.D. thesis, Univ. Delaware, Newark (1959).
14. ———, and A. B. Metzner, *A.I.Ch.E. J.*, **5**, 189 (1959).
15. Farmer, R. C., M.S. thesis, Univ. Delaware, Newark (in preparation), data obtainable from reference *16*.
16. Friend, P. S., M.S. thesis, Univ. Delaware, Newark (1958).
17. Friend, W. L., M.S. thesis, Univ. Delaware, Newark (1957).
18. ———, and A. B. Metzner, *A.I.Ch.E. J.*, **4**, 393 (1959).
19. Haines, R. C., B.S. thesis, Univ. Delaware, Newark (1957).
20. Hanks, R. W., Ph.D. thesis, Univ. Utah, Salt Lake City (1960).
21. ———, and E. B. Christiansen, *A.I.Ch.E. J.*, **7**, 519 (1961).
22. Hanks, R. W., *ibid.*, **9**, 45 (1963).
23. *Ibid.*, 306 (1963).
24. Jensen, G. E., Ph.D. thesis, Univ. Utah, Salt Lake City (1963).

25. Johnson, H. A., J. P. Hartnett, and W. J. Clabaugh, *Trans. Am. Soc. Mech. Engrs.*, **76**, 513 (1954).
26. Johnson, M. M., Ph.D. thesis, Univ. Utah, Salt Lake City (1958).
27. Knudsen, J. G., and D. L. Katz, "Fluid Dynamics and Heat Transfer," McGraw-Hill, New York (1958).
28. Kreith, Frank, and M. Summerfield. *Trans. Am. Soc. Mech. Engrs.*, **72**, 869 (1950).
29. Kroll, C. L., Sc.D. thesis, Massachusetts Inst. Tech., Cambridge (1951).
30. Kuznetsov, M. D., and V. M. Leonencke, *Khim. Nauka Prom.*, **4**, 406 (1959).
31. Levêque, J., *Ann. Mines*, **12**, 201 (1928).
32. Merkel, W., *Beschefte Gesundheits-Ingenieur*, Riehe II, Hefte **14**.
33. Metzner, A. B., in "Advances in Chemical Engineering," Vol. I, Academic Press, New York (1956).
34. ———, R. D. Vaughn, and G. L. Houghton, *A.I.Ch.E. J.*, **3**, 92 (1957).
35. Metzner, A. B., and W. L. Friend, *Can. J. Chem. Eng.*, **36**, 235 (1958).
36. Metzner, A. B., and P. S. Friend, *Ind. Eng. Chem.*, **51**, 879 (1959).
37. Morris, F. H., and W. G. Whitman, *ibid.*, **20**, 234 (1928).
38. Orr, C., Jr., and J. M. Dalla Valle, *Chem. Eng. Progr. Symposium Ser. No. 9*, **50**, 29 (1954).
39. Perry, J. H., ed., "Chemical Engineers' Handbook," 3 ed., p. 383, McGraw-Hill, New York (1950).
40. Petersen, A. W., Ph.D. thesis, Univ. Utah, Salt Lake City (1960).
41. Progress Report of Committee of the Sanitary Engineering Div., *Proc. A. S. C. E.*, **55**, 1773 (1929).
42. Rabinowitsch, B., *Z. Phys. Chem.*, **A145**, 1 (1929).
43. Raniere, F. D., B.S. thesis, Univ. Delaware, Newark (1957).
44. Reichardt, H., *Natl. Advisory Comm. Aeronaut. Tech. Mem. 1408* (1957).
45. Ryan, N. W., and M. M. Johnson, *A.I.Ch.E. J.*, **5**, 433 (1959).
46. Salt, D. L., N. W. Ryan, and E. B. Christiansen, *J. Colloid Sci.*, **6**, 146 (1951).
47. Sieder, E. N., and G. E. Tate, *Ind. Eng. Chem.*, 28, 1429 (1936).
48. Sherwood, T. K., D. D. Kiley, and G. E. Mangsen, *ibid.*, **24**, 273 (1932).
49. Stevens, W. E., Ph.D. thesis, Univ. Utah, Salt Lake City (1953).
50. Tau, Fan-Sheng, M.S. thesis, Univ. Utah, Salt Lake City (1964).
51. Thomas, D. G., paper presented at A.I.Ch.E. Salt Lake City meeting (September, 1958).
52. ———, *A.I.Ch.E. J.*, **6**, 631 (1960).
53. Wilhelm, R. H., D. M. Wroughton, and W. F. Loeffel, *Ind. Eng. Chem.*, **31**, 622 (1939).
54. Winding, C. C., G. P. Baumann, and W. L. Kranich, *Chem. Eng. Progr.*, **43**, 527 613 (1947).

Manuscript received February 10, 1965; revision received October 6, 1965; paper accepted October 7, 1965. Paper presented at A.I.Ch.E. Los Angeles meeting.

Dynamic Characteristics of Perforated Distillation Plates Operating at Low Loads

B. K. C. CHAN and R. G. H. PRINCE

University of Sydney, Sydney, Australia

Analysis of the equations describing the instantaneous vapor and liquid flow through the holes of perforated distillation plates at low loads shows that periodic and stable pressure oscillations will always be set up between plates. These oscillations are expected to have amplitudes of the order of 0.1 in. of water and frequencies of a few cycles per second, values which are in accord with observation and which may be used as the basis for a model from which the seal point of the plates may be predicted.

In a recent paper (*11*) the authors have discussed the prediction of the "seal point" of perforated distillation plates (such as the plate illustrated in Figures 1 and 2 of reference *11*) which they take as corresponding to the minimum load of these plates. They have defined the seal point as the vapor rate required to just maintain the liquid level on a plate at the weir height, for a given rate of liquid supplied to the plate. This point is then to be distinguished from the "weep point," generally defined as the vapor rate required to prevent any liquid from flowing ("weeping") through the plate perforations.

At the seal point all liquid fed to the plate weeps through the perforations. An increase in vapor rate leads to a decreasing proportion of the total liquid flow weeping (until the weep point is attained), while a decrease in the vapor rate will lead to a rapid decrease in liquid height on the plate, that is, the liquid seal on the plate will be lost. The points may be identified on a plot of vapor pressure drop against vapor rate for a fixed liquid rate (or fixed ratio, liquid:vapor) (a typical plot is shown in Figure 1). At *A* no liquid seal exists on the plate; *B* corresponds to the seal point and a higher vapor rate; *C* is the weep point.

The region between the seal point and the weep point may be referred to as the "weeping range." The overall pressure drop shows little or no increase over this range. Beyond the weep point, however, each hole must carry an increasing vapor load; hence the pressure drop will increase more rapidly. In the weeping range, the overall mass transfer efficiency will be reasonable, unless a high proportion of liquid weeps through a plate on which the

R. G. H. Prince is with the University of Queensland, St. Lucia, Brisbane, Australia.